

# **Electronic Supporting Information for**

## **Nanoporous Silicon Photocathodes with [Co] Molecular**

### **Catalyst for Enhanced Solar-Driven Hydrogen Generation**

Luo-Han Xie,<sup>†</sup> Fentahun Wondu Dagnaw,<sup>†</sup> Ming-Ming Yao, Yi-Jing Chen, Jing Chen, Jing-Xin Jian,<sup>\*</sup> Qing-Xiao Tong<sup>\*</sup>

<sup>†</sup>L.-H. Xie and F. W. Dagnaw contributed equally to this work.

College of Chemistry and Chemical Engineering, Key Laboratory for Preparation and Application of Ordered Structural Material of Guangdong Province, and Guangdong Provincial Key Laboratory of Marine Disaster Prediction and Prevention, Shantou University, Shantou, Guangdong, 515063, China.

E-mail: [jxjian@stu.edu.cn](mailto:jxjian@stu.edu.cn), [qxtong@stu.edu.cn](mailto:qxtong@stu.edu.cn)

## 1. Experimental Details

### 1.1. Reagents and Instrumentation

Unless otherwise stated, all reagents used for preparation of intermediates as well as cobalt-oxime catalyst were used as received without any further purification. Bruker AV spectrometer operating at 400 and 100 MHz was used to measure  $^1\text{H}$  NMR spectra and  $^{13}\text{C}$  NMR spectra respectively using TMS ( $\sigma = 0.00$  ppm) as an internal standard.

Full-scale characterizations of [Co] catalyst as well as silicon wafers were performed by several instrumental techniques. The elemental composition of the prepared catalyst was analyzed using an energy dispersive spectroscopy (EDS) coupled with FESEM by point and surface scanning. The crystal structure was analyzed by X-ray diffraction (D8 ADVANCE from Bruker, Germany) with the scanning range of 4 to 80 degrees and scanning speed of 10 degrees per minute. The light absorption of the silicon electrode was measured by using Perkin Elmer's Lambda750 UV-vis-NIR with a scanning range of 1200 nm to 400 nm. Elemental analysis of the catalyst was performed by using X-ray photoelectron spectroscopy (Thermo ESCALAB 250Xi X-ray photoelectron spectroscopy) analyzer with a test energy range of 0 to 5000 eV by calibrating the binding energy at C1s 284.8 eV using monochrome Al K with a power of 150W  $\alpha$  ( $h\nu=1486.6$  eV) as the emission source. Functional group identification of cobalt oxime catalyst was performed by Fourier transform infrared spectrometer (FT-IR, Nicolet iS50. Nicolet iS50) and the signals of the functional groups were collected with the wavenumber range of 4000-400  $\text{cm}^{-1}$ .

### 1.2. Fabrication of Si electrodes

#### 1.2.1. Process of Si electrodes

Flat Si (*f*-Si) wafers was cleaned by RCA standard cleaning method. The Si wafer was immersed in acetone and sonicated for 5 minutes to remove surface organic impurities. The wafer was rinsed several times with ethanol and deionized water repeatedly. The cleaned *f*-Si was immersed in mixed solution of hydrogen peroxide, ammonia water and deionized water ( $v/v/v = 1:1:5$ ) at 75 °C for 5 minutes to remove organic matter and metallic compounds from Si surface. After rinsing with ethanol and deionized water, *f*-Si was immersed in mixed solution of hydrogen peroxide, hydrochloric acid and deionized water ( $v/v/v=1:1:6$ ) at 75 °C for 5 minutes to remove metal ions and some hydroxides. Following, Si wafer was rinsed with deionized water and 5% hydrofluoric acid and blown dry under a  $\text{N}_2$  flow. Si photocathode was fabricated with ohmic contact of 200 nm Al on the backside and connect to Cu tape. Fix Si wafer on a plastic plate and

seal the edges with epoxy resin. Only the front surface of Si is exposed to electrolyte and light for etching and PEC measurements. The whole cleaning procedure is shown in the Figure S1.

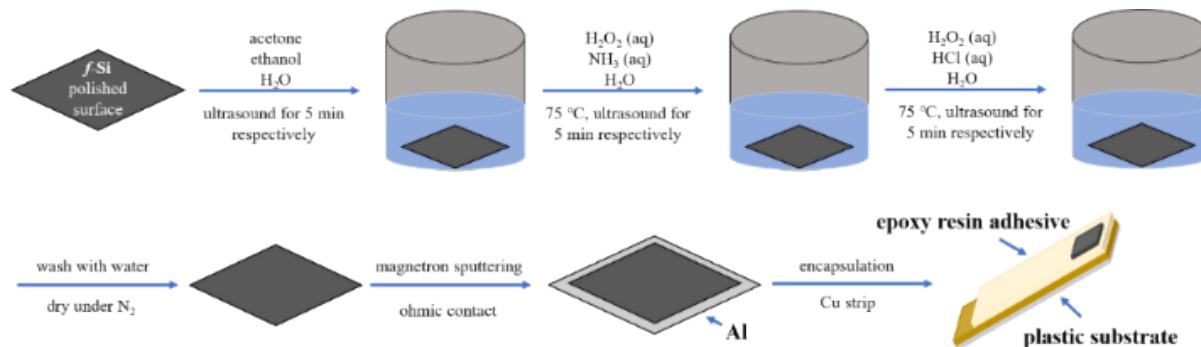


Figure S1. Schematic diagram of cleaning and packaging process of Si electrodes.

### 1.2.2. Ohmic contact of Si electrodes

200 nm Al film on the back surface of the Si wafer through magnetron sputtering. The working conditions of deposition was controlled as 0.001 Pa for background vacuum value, 0.5 Pa for working pressure, 80 W for target material, 40 min for sputtering time and about 200 nm of deposition thickness. A linear current voltage curve of ohmic contact test (Figure S2) prove that a good ohmic contact was formed between Al film with Si wafer.

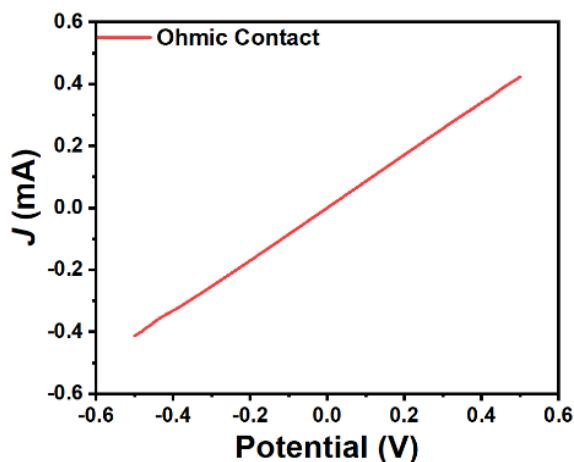


Figure S2. The current-voltage curve of Si electrode with 200 nm Al deposited on the back.

### 1.3. Surface Morphology and Structure Characterization

Surface of the Si electrodes were characterized by scanning electron microscopy (SEM) and

field emission scanning electron microscope (FESEM). The samples were fixed on the conductive tape and use Pt spraying method to improve the conductivity of samples. The surface morphology of the sample was taken using different scanning electron microscope probes.

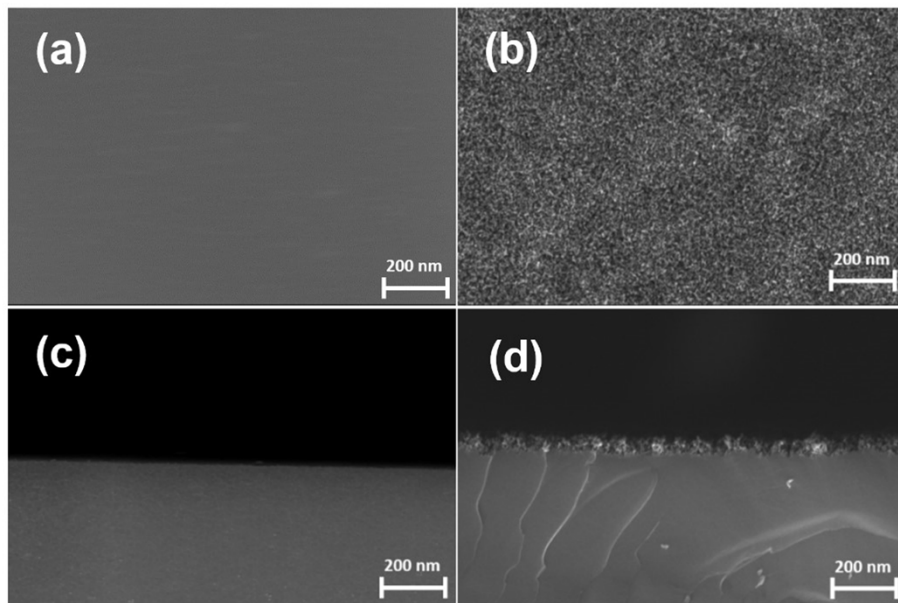


Figure S3. Top-view SEM images of *f*-Si (a) and *b*-Si (b); cross-view SEM images of *f*-Si (c) and *b*-Si (d).

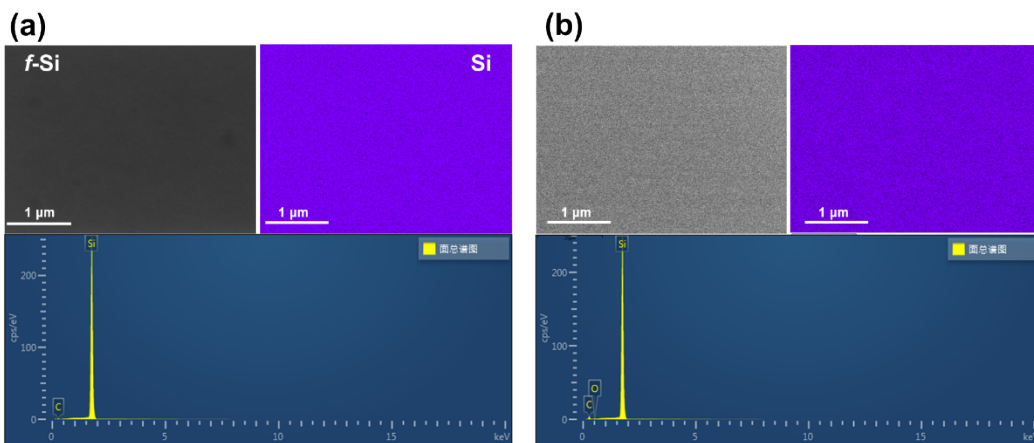


Figure S4. SEM images and the related EDS elements mapping of *f*-Si (a) and *b*-Si (b).

## 1.4. Synthesis of cobalt oxime catalyst

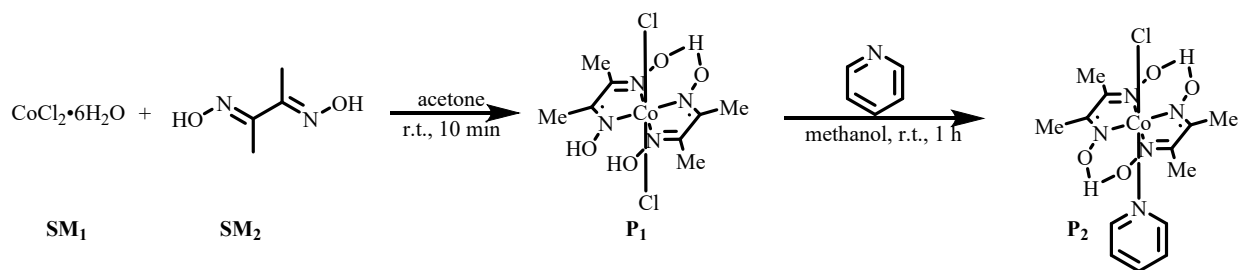


Figure S5. Synthesis route for Co(dmgh)<sub>2</sub>(py)Cl catalyst

### 1.4.1 Preparation of intermediate product (P<sub>1</sub>)

The intermediate product (P<sub>1</sub>), Co(dmgh)<sub>2</sub>(dmgh)Cl<sub>2</sub>, was prepared according to the literature.<sup>[1]</sup> Hence, the mixture of cobalt chloride hexahydrate (SM<sub>1</sub>, 5 g, 21 mmol, 1 equiv.) and dimethylglyoxime (SM<sub>2</sub>, 4.9 g, 42.2 mmol, 2.01 equiv.) in acetone (150 mL) was stirred for 10 minutes. After the completion of the reaction, the solution was filtered and the collected filtrate was stirred overnight to get green solid precipitate. The solid product was filtered and dried in an oven. (P<sub>1</sub>, 75%)

### 1.4.2 Preparation of cobalt catalyst (P<sub>2</sub>)

The Co(dmgh)<sub>2</sub>(py)Cl catalyst was prepared based on the methods from the literature.<sup>[1]</sup> The P<sub>1</sub> (3.3 g, 9 mmol, 1 equiv.) was added to a reaction flask containing 50 mL of methanol. Then, pyridine (0.7 g, 9 mmol, 1 equiv.) was added and stirred for 1 hour to get brown solid. The solid precipitate was then separated by suction filtration and washed with ether (10 mL) several times. Finally, the remaining solid was dried in an oven to get the desired product Co(dmgh)<sub>2</sub>pyCl (P<sub>2</sub>, 65%). The formation of the product was confirmed by <sup>1</sup>H NMR and <sup>13</sup>C NMR. <sup>1</sup>H NMR (400 MHz, Methylene Chloride-*d*<sub>2</sub>): δ = 8.25-8.18 (m, 2H), 7.72 (tt, J = 7.6, 1.5 Hz, 1H), 7.30-7.21 (m, 2H), 2.39 (s, 12H). <sup>13</sup>C NMR (101 MHz, Methylene Chloride-*d*<sub>2</sub>) δ 152.68, 150.93, 138.89, 125.66, 12.76.

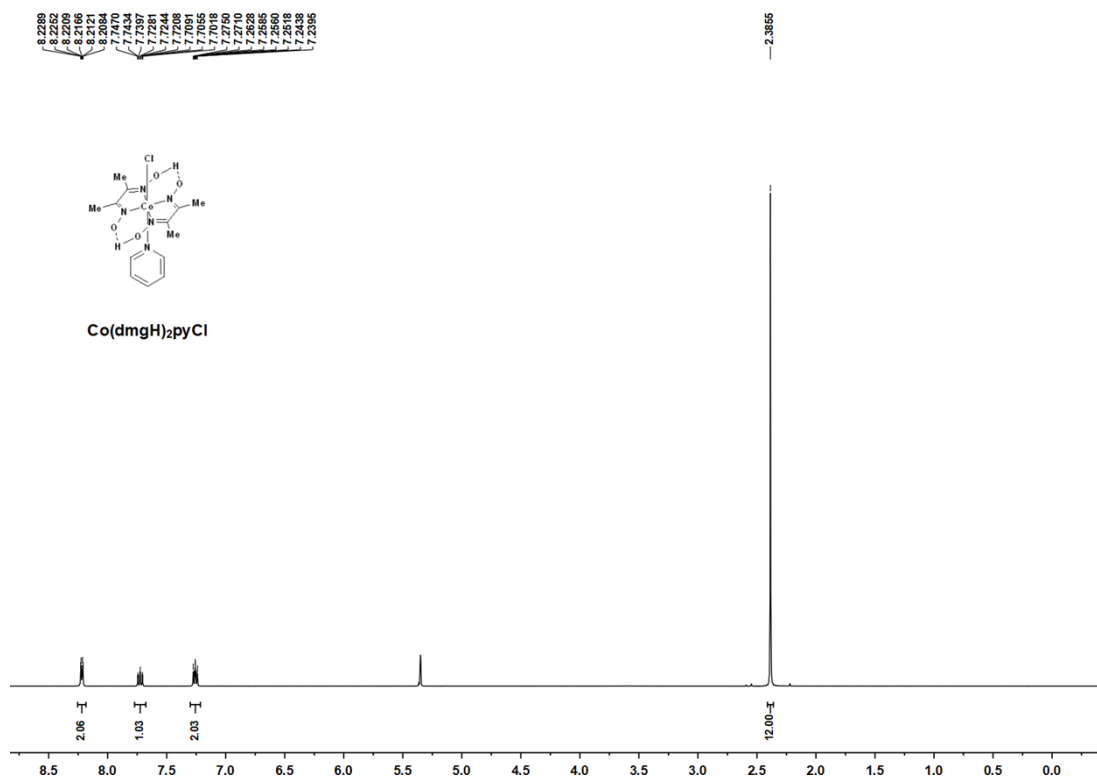


Figure S6.  $^1\text{H}$  NMR spectrum of  $\text{Co}(\text{dmgH})_2(\text{py})\text{Cl}$  in  $\text{d}^2\text{-DCM}$ .

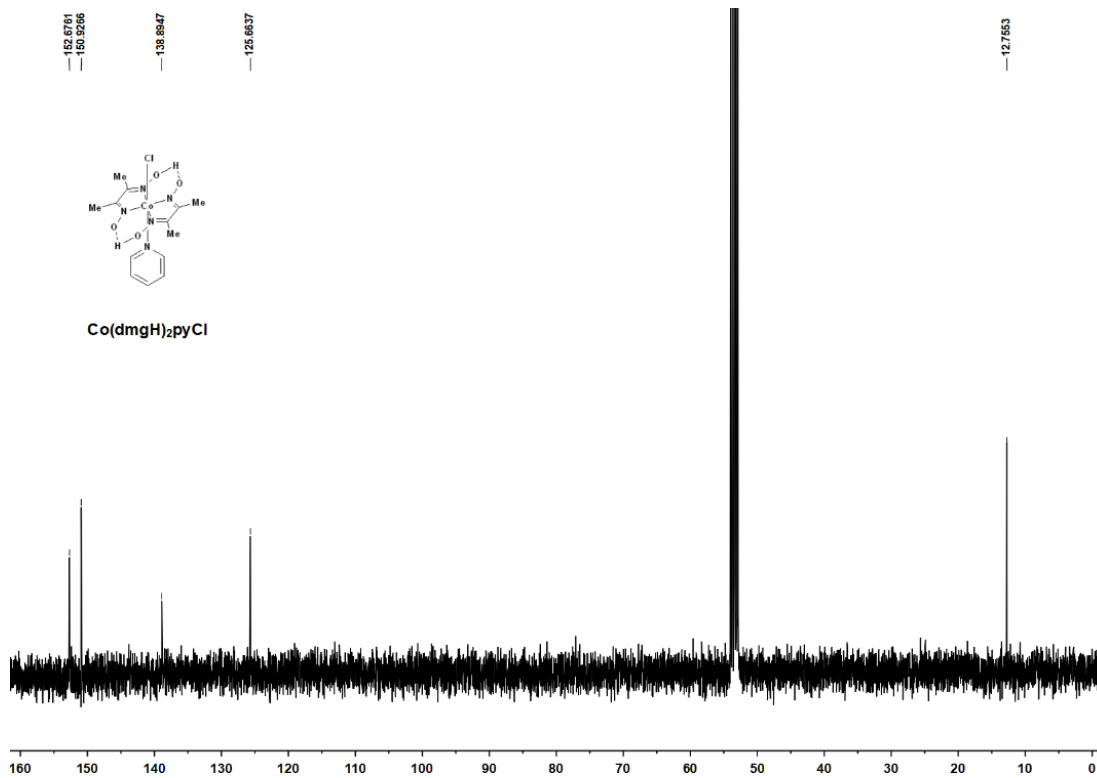


Figure S7.  $^{13}\text{C}$  NMR spectrum of  $\text{Co}(\text{dmgH})_2(\text{py})\text{Cl}$  in  $\text{d}^2\text{-DCM}$

### 1.5. Deposition of [Co] catalyst on *b*-Si

The *b*-Si photoelectrode with nanoporous surface was prepared by electrochemical etching as shown in Figure S1. The etching process was performed in a potentiostat by applying a constant current for 30 minutes. And hence a silicon electrode to be etched was immersed in a 5 wt% HF solution using a Pt electrode as the counter electrode and a two-electrode system. The etched silicon photoelectrode was washed several times with deionized water to remove the HF attached to the electrode surface, and then dried under nitrogen. After the electrode is dried, it was placed on the sample stage of the spin coating instrument and vacuum pump was used to fix the silicon electrode. Finally, 0.1 mL of the ultrasonically dispersed solution of 0.2 mg of cobalt catalyst, 0.5 mL of 5 wt% Nafion solution was dropped out carefully on to the surface of the etched silicon electrode each time by fixing the set the rotational speed to 100 rpm, and allowed to dry at room temperature for 60 min.

### 1.6. Photoelectrochemical measurements

All PEC measurements were conducted in a three-electrode electrolytic cell system under nitrogen at 25 °C, using a prepared silicon-based photocathode (1 cm<sup>2</sup>), Pt sheet electrode and Ag/AgCl (saturated KCl) as a working electrodes, counter electrodes, and reference electrodes respectively. The standard simulated solar light (AM1.5G, 100 mW cm<sup>-2</sup>) was used as a light source for hydrogen production from water splitting under PEC system. Prior to PEC measurement, the sealed electrolytic cell was bubbled with high purity nitrogen (99.999%) for 30 minutes to promote deoxidation of the electrolyte solution (0.5 M H<sub>2</sub>SO<sub>4</sub>, pH: 0.2). The LSV curves of different types of Si-based photocathodes were measured under continuous illumination and switching lamp illumination at a scanning rate of 30 mV/s.

The electrochemical impedance spectroscopy (EIS) was measured using an electrochemical workstation in a dark box with a scanning frequency of 1000 kHz to 1 Hz and an amplitude of 10 mV at 0 V<sub>RHE</sub>. On the other hand, the amount of H<sub>2</sub> generated by a Si-based photocathode system was measured using a gas chromatograph (GC7920). The Faraday efficiency was calculated from the ratio of the amount of H<sub>2</sub> from the working electrode and the amount of H<sub>2</sub> from Pt electrode at the same current, assuming a Faraday efficiency of 100% for the Pt electrode. The potential measured in all experiments was converted to the potential corresponding to RHE by the following equation:  $E_{(RHE)} = E_{(Ag/AgCl)} + E^{\ominus}_{(Ag/AgCl)} + 0.059 \times \text{pH}$  ( $E^{\ominus}_{(Ag/AgCl)} = 0.197 \text{ V}, 25^{\circ}\text{C}$ ).

**Table S1.** Recent works using Si-based photocathode with molecular HER catalysts for water splitting.

no.	photocathode	$V_{\text{on}}$ ( $V_{\text{RHE}}$ )	$J_{\text{sat.}}$ ( $\text{mA cm}^{-2}$ )	$J_{0V}$ ( $\text{mA}\cdot\text{cm}^{-2}$ )	Ref.
1	Si/IO-TiO <sub>2</sub> /H <sub>2</sub> ase	0.35	/	-0.7	<i>Angew. Chem. Int. Ed.</i> , <b>2018</b> , 57, 10595. <sup>[2]</sup>
2	Si/TiO <sub>2</sub> /NiP, CoP <sub>3</sub>	0.4	/	-0.43	<i>Chem. Sci.</i> , <b>2017</b> , 8, 5172. <sup>[3]</sup>
3	Si/NiATSM	0.03	-30	-1	<i>Chem. Commun.</i> , <b>2019</b> , 55, 9440. <sup>[4]</sup>
4	b-Si/[Co]	0.31	-23.9	-4.15	This work

**Table S2.** Fitting results of the EIS data for *f*-Si, *f*-Si/[Co], *b*-Si and *b*-Si/[Co] photocathodes.

Sample	$R_s$ ( $\Omega\cdot\text{cm}^2$ )	$R_{\text{bulk}}$ ( $\Omega\cdot\text{cm}^2$ )	$R_{\text{ct}}$ ( $\Omega\cdot\text{cm}^2$ )
<i>f</i> -Si	15	23	2790000
<i>f</i> -Si/[Co]	26	42	17750
<i>b</i> -Si	18	26	46500
<i>b</i> -Si/[Co]	12	36	143



## 1.7. HER mechanism of $\text{Co}(\text{dmgH})_2(\text{py})\text{Cl}$

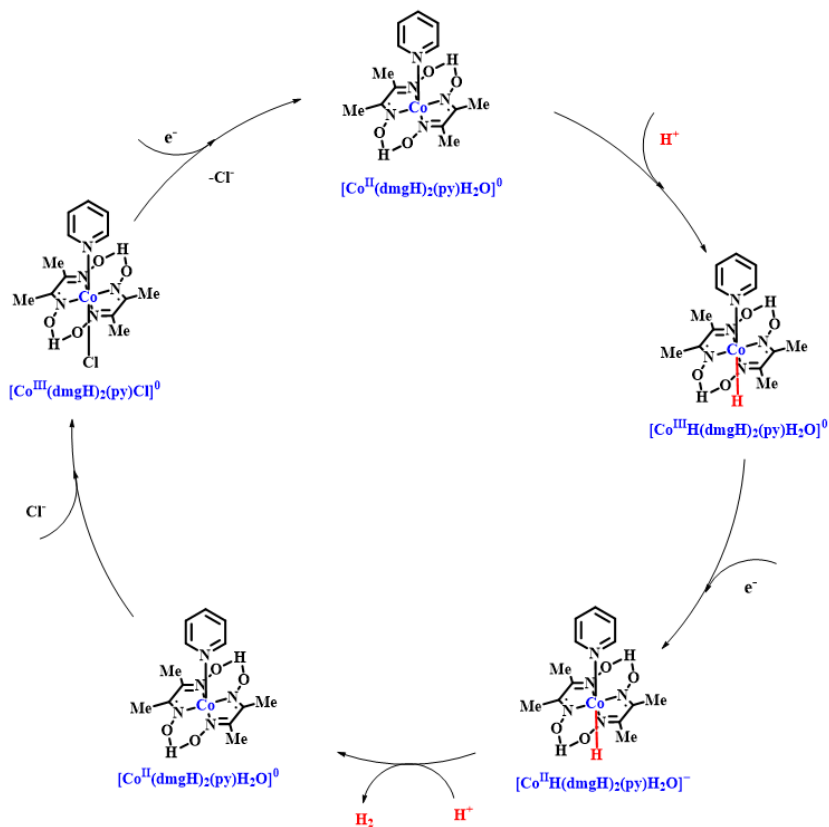


Figure S8 HER mechanism of  $\text{Co}(\text{dmgH})_2(\text{py})\text{Cl}$ .

$[\text{Co}^{\text{III}}(\text{dmgH})_2(\text{py})\text{Cl}]$  complex gets an electron and evolves into  $[\text{Co}^{\text{II}}(\text{dmgH})_2(\text{py})\text{H}_2\text{O}]^0$  (or  $[\text{Co}^{\text{II}}]^0$ ) as the resting precursor for the catalytic HER reaction. The state of  $[\text{Co}^{\text{II}}]^0$  is reduced to produce the  $[\text{Co}^{\text{I}}(\text{dmgH})_2(\text{py})(\text{H}_2\text{O})]$  species (or  $[\text{Co}^{\text{I}}]^-$ ).  $\text{H}_2\text{O}$  molecule points towards the Co center with one of its H atoms resulting in the  $[\text{Co}^{\text{III}}\text{H}(\text{dmgH})_2(\text{py})(\text{H}_2\text{O})]^0$  species (or  $[\text{Co}^{\text{III}}\text{H}]^0$ ). After receiving one electron to form the  $[\text{Co}^{\text{II}}\text{H}(\text{dmgH})_2(\text{py})(\text{H}_2\text{O})]^-$  species (or  $[\text{Co}^{\text{II}}\text{H}]^-$ ). The  $\text{H}_2$  molecule is produced upon relaxation when the second proton was added, and the complex returns to the  $[\text{Co}^{\text{II}}]^0$  state. Finally, the  $[\text{Co}^{\text{II}}]^0$  returns to  $[\text{Co}^{\text{III}}(\text{dmgH})_2(\text{py})\text{Cl}]^0$  complex (Figure S8).

## References

- [1] E. Oswald, A. L. Gaus, J. Kund, M. Kullmer, J. Romer, S. Weizenegger, T. Ullrich, A. K. Mengele, L. Petermann, R. Leiter, P. R. Unwin, U. Kaiser, S. Rau, A. Kahnt, A. Turchanin, M. von Delius, C. Kranz, *Chem. Eur. J.*, **2021**, *27*, 16896-16903.
- [2] D. H. Nam, J. Z. Zhang, V. Andrei, N. Kornienko, N. Heidary, A. Wagner, K. Nakanishi, K. P. Sokol, B. Slater, I. Zebger, S. Hofmann, J. C. Fontecilla-Camps, C. B. Park, E. Reisner, *Angewandte Chemie International Edition*, **2018**, *57*, 10595-10599.
- [3] J. J. Leung, J. Warnan, D. H. Nam, J. Z. Zhang, J. Willkomm, E. Reisner, *Chem Sci*, **2017**, *8*, 5172-5180.
- [4] S. Gulati, O. Hietsoi, C. A. Calvary, J. M. Strain, S. Pishgar, H. C. Brun, C. A. Grapperhaus, R. M. Buchanan, J. M. Spurgeon, *Chem Commun*, **2019**, *55*, 9440-9443.